

Original Research Article

<https://doi.org/10.20546/ijcmas.2020.901.185>

Downscaling daily precipitation over the Upper Shivrath basin: A comparison of three statistical downscaling techniques

Vijay Kumar Singh* and Devendra Kumar

Department of Soil and Water Conservation Engineering, Govind Ballabh Pant University of Agriculture and Technology, Pantnagar, Uttarakhand – 263145, India

*Corresponding author

ABSTRACT

Keywords

Delta method, quantile mapping method and empirical quantile mapping method, downscale

Article Info

Accepted:
15 December 2019
Available Online:
20 January 2020

In this study, three different statistical downscale method namely delta method (DM), quantile mapping method (QMM) and empirical quantile mapping method (EQMM) are compare to downscale precipitation for Upper Shivrath basin. Model for Interdisciplinary Research on Climate 5 (MIRCO5) simulation model is used for future Representative Concentration Pathways (RCP) scenarios (RCP4.5) to project decadal changes in precipitation across eighteen selected stations of Upper Shivrath basin. Three decades are selected for future prediction viz. 2020–2039, 2040–2059, 2060–2079 and 2080–2099 and are compared decadal variabilities with period 1990–2013. Delta method is accurately downscale precipitation from Model for Interdisciplinary Research on Climate (MIRCO5) model for future Representative Concentration Pathways (RCP) scenarios (RCP4.5) to project decadal changes in precipitation across eighteen selected stations of Upper Shivrath basin as compare to quantile mapping and empirical quantile mapping methods. The downscale precipitation of Upper Shivrath basin from Interdisciplinary Research on Climate (MIRCO5) model for 2020–2039, 2040–2059, 2060–2079 and 2080–2099 scenarios are observed decrease trend in future.

Introduction

Chhatishgarh state has a great variety of climates, mainly given its vast latitudinal extent, its complex orography. These features in complex combination with remote forcing contribute to define the climates of Shivrath basin and their variability. With such a varied range of climate regions and in the context of

climate change, it is then essential to develop tools to study the regional climate and its possible evolution. Global climate models (GCM) have been designed to describe large-scale climate characteristics and the potential evolution of climate under future emission scenarios (Meehl *et al.*, 2007). However, GCM still show major deficiencies when it comes to representing small-scale processes

that may condition the regional climate (Bettolli & Penalba, 2014; Maenza, AgostaScarel, & Bettolli, 2017; Silvestri & Vera, 2008). Therefore, in order to generate climate information at a regional or local scale, it is necessary to apply downscaling techniques to relate large-scale information provided by GCM to the regional-scale climate information needed to assess impacts and decision-making. To obtain high-resolution projections, two approaches are commonly used. Dynamical downscaling techniques are based on regional climate models (RCMs) that simulate regional climate processes with a greater spatial resolution, using GCM fields as boundary conditions (Giorgi & Mearns, 1991; Rummukainen, 2010). On the other hand, empirical statistical downscaling (ESD) methods generate climate information at local scale or with a greater resolution than that achieved by GCMs by means of empirical/statistical relationships between large-scale atmospheric variables and local climate (Wilby *et al.*, 2004). Comparative studies between RCM and ESD simulations suggest that both approaches show comparable skills to represent regional climate characteristics (Huth *et al.*, 2015; Menéndez *et al.*, 2009), adding value to GCM simulations.

Therefore, efforts to develop and validate different regional climate modelling techniques are of great importance not only to better understand the climate system, but also to generate detailed and tailored climate information. Therefore, the objective of this study is to calibrate and validate the analogue method as a technique to downscale daily precipitation of Upper Shivnath basin. This region in particular was selected mainly because it extends over the most productive agricultural area, whose predominant activities are extensive rainfed agriculture and livestock farming.

Materials and Methods

The Mahanadi river is one of the major inter-state east flowing perennial rivers in peninsular India. Number of tributaries viz. Shivnath, Jonk, Hamp, Pairi and Kharun joins Mahanadi river. The river basin is sub divided into three sub-basins viz. upper, middle and lower Mahanadi basins. The upper basin and part of middle Mahanadi basin falls in Chhattisgarh state while the lower basin falls under Odisha state. The total catchment area of the Upper Mahanadi Basin is 29,759 Km² and it covers the districts of Bilaspur, Kawardha, Raipur, Bemetara, Dhamtari, Kabirdham, Rajnandgaon and Durg.

On scrutiny of all the watersheds of sub-basin of upper Mahanadi Basin, the Upper Shivnath river basin is selected for the current study. The Upper Shivnath river originates near village Panabaras in the Rajnandgaon District. The Upper Shivnath basin is located between latitude 20⁰ 16' N to 22⁰ 41' N and Longitude 80⁰ 25' E to 82⁰35' E. The Basin area of river up to confluence with the Mahanadi River is 16786 Km². The river traverses a length 380 Km. The main tributaries of Upper Shivnath river are Tandula, Kharun, Arpa, Hamp, Agar and Maniyari Rivers. The Upper Shivnath river is mainstream of the Shivnath river and its outlet is at Sigma. The Shivnath river is situated at the upper most boundary of the Mahanadi basin and most of the upland area with steep slopes causes losses of soil, providing essential reasoning for the selection of the watershed for this study. The northern and western parts are surrounded by Maikal mountain ranges of Satpura. Here the highest peak is Kesmarda in Maikal Mountain, which is 978 m high, while the lowest elevation of the watershed is 237 m. The central east and southern part of the Shivnath basin is plain, whereas the northern and western part is mountainous. The climate of upper Shivnath is temperate, where the maximum

temperature in summer is 42⁰C and the minimum temperature in winter goes to the lowest of 15⁰C. The overall climate of the area can be classified as sub-humid tropical. Major crops grown in the area are paddy (rice), maize, soybean in Kharif (monsoon season) and chick pea and sugarcane in Rabi (winter season).

Data acquisition

Meteorological data

The daily rainfall data for 24 years (1990 - 2013) is acquired from Hydrometeorology Division of Central Water Commission (CWC) and Meteorological Centre of Indian Meteorological Department, Raipur, Chhattisgarh. Due to unavailability of location specific data of other meteorological observations, the global and high resolution meteorological data such as precipitation (mm) is downloaded from Climate Forecast System Reanalysis (CFSR) site (<https://rda.ucar.edu/pub/cfsr.html>). Long term data based on availability were also collected from the Hydrology Data Center, Department of Water Resources, Govt. of Chhattisgarh for two rainfall gauging stations namely Amdi and Singdai, which lies within Kharun and Upper Shivrath basin. The elevation, location and list of meteorological stations, which are acquired from different sources. respectively are given in Table 1.

Downscaling concept

Raw outputs from General Circulation Model (GCM) simulations are inadequate for assessing the impact of hydrological, agricultural, and other studies. Due to inadequate and too coarse spatial scale of GCMs outputs (typically 250 km), scientists have to perform different methods to solve this problem, and therefore, downscaling methods have been used. Downscaling

bridged the gap between coarse and fine scale climatic data. Downscaling can be performed on spatial and temporal aspects of climate projections. Spatial downscaling methods are used to extract finer-resolution spatial climate information from coarser-resolution GCM output.

Downscaling concept is classified into two types downscaling namely dynamical downscaling (DD) and statistical downscaling (SD). The dynamical downscaling is very computationally intensive, very complex, requires substantial computational resources, making its use in impact studies limited and essentially impossible for multi-decade simulations. Therefore, statistical downscaling is used in present study. In general, the statistical methods can be divided into three categories: regression (transfer function) method, stochastic weather generator and weather pattern schemes. There are a numerous number of statistical downscaling methods. One of the most popular and common of them is bias correction (BC) that has been applied extensively for impact assessment and employed in climate change studies in all over the world. These methods include many statistical techniques that is run with various application in every part of the world, but almost many of these applications with CMIP5 outputs are difficult to run by researchers. In the present studied, three methods of statistical downscaling namely delta method (DM), quantile mapping method (QMM) and empirical quantile mapping method (EQMM) are used. All of them are explained in the following paragraphs. As presented in Eq. 3.16 the precipitation of GCM data are downscaled.

$$PCP_{SD} = PCP_{GCMrcp} \times \frac{PCP_{obs}}{PCP_{GCMhist}} \dots(1)$$

where, PCP_{SD} Delta is downscaled data of precipitation, PCP_{obs} refers the average observed and $PCP_{GCMhist}$, represents to GCM

mean simulation historical data of precipitation, Subscript *GCMrcp* represents the *GCM* and *RCP* outputs over the future period and subscript *obs* represents the observation values.

In the equation of quantile mapping and empirical quantile mapping methods, the modelled probabilistic distribution to observed probabilistic distribution is calculated.

$$P_t^{Eval} = InvCDF_{Pt-cal}^{obs} (CDF_{Pt-cal}^{hist} \times P_{t-RCP}^{GCM}) \dots(2)$$

$$P_t^{Predict} = InvCDF_{Pt-Hist}^{obs} (P_{t-RCP}^{GCM}) \dots(3)$$

$$P_t^{Eval} = InvECDF_{Pt-cal}^{obs} (ECDF_{Pt-cal}^{hist} \times P_{t-RCP}^{GCM}) \dots(4)$$

$$P_t^{Predict} = InvECDF_{Pt-Hist}^{obs} (P_{t-RCP}^{GCM}) \dots(5)$$

Where, CDF and ECDF are the cumulative distribution function and empirical cumulative distribution function of the observation and historical data in time period (t), P_t is precipitation of GCM, predicted and evaluation data in time period (t).

Model performance evaluation

Root mean square error

$$RMSE = \sqrt{\frac{\sum_{i=1}^n (Y_t - Y_p)^2}{n}} \dots (6)$$

Where Y_t is observed data series, Y_p is predicted data series, n is number of observations.

Correlation coefficient

$$r = \left[\frac{\sum_{i=1}^n \{(Y_t - \bar{Y}_t)(Y_p - \bar{Y}_p)\}}{\sqrt{\sum_{i=1}^n (Y_t - \bar{Y}_t)^2} \sqrt{\sum_{i=1}^n (Y_p - \bar{Y}_p)^2}} \right] \dots (7)$$

Where \bar{Y}_t is average of the observed data series and \bar{Y}_p is average of predicted data series.

Coefficient of efficiency

$$CE = 1 - \frac{\sum_{i=1}^n (Y_t - Y_p)^2}{\sum_{i=1}^n (Y_t - \bar{Y}_t)^2} \dots (8)$$

Results and Discussion

The observed dataset for baseline period (1990-2013) was collected from department of agrometeorology, Indra Gandhi Krishi Vishwavidyalaya, Raipur, Chhatishgarh, India and regional office of IMD and CWC, Raipur, Chhatishgarh, India. Model for Interdisciplinary Research on Climate 5 (MIRCO5) simulation model from Coupled Model Inter Comparison Project Phase 5 (CMIP5) model was used for future Representative Concentration Pathways (RCP) scenarios (RCP4.5) to project decadal changes in precipitation across eighteen selected stations of Upper Shivrath basin. Four decades were selected for future prediction viz. 2020–2039, 2040–2059, 2060–2079 and 2080-2099 and decadal variabilities were compared with period 1990–2013. In the present study, three methods of statistical downscaling namely delta method (DM), quantile mapping method (QMM) and empirical quantile mapping method (EQMM) are used. The results of different downscaling techniques are presented in Table 2. The delta method estimated the best values of the values of RMSE (10.056), r (0.647) and NSE (0.35) for Site_1, RMSE (5.810), r (0.859) and NSE (0.728) for Site_2, RMSE (7.590), r (0.725) and NSE (0.513) for Site_3, RMSE (5.812), r (0.859) and NSE (0.690) for Site_4, RMSE (5.819), r (0.863) and NSE (0.0.735) for Site_5, RMSE (5.110), r (0.836) and NSE (0.680) for Site_6, RMSE (7.930), r (0.779) and NSE (0.595) for Site_7, RMSE (6.364), r (0.846) and NSE (0.709) for Site_8, RMSE (6.933), r (0.736) and NSE (0.409) for Site_9, RMSE (7.592), r (0.776) and NSE (0.591) for Site_10, RMSE (7.411), r (0.787) and NSE (0.606) for Site_11, RMSE (7.183), r (0.827) and NSE (0.563) for Site_13,

RMSE (7.183), r (0.823) and NSE (0.670) for Site_14, RMSE (7.411), r (0.787) and NSE (0.390) for Site_15, RMSE (8.810), r (0.703) and NSE (0.308) for Amdi, RMSE (9.352), r (0.537) and NSE (0.351) for Raipur, RMSE (8.961), r (0.725) and NSE (0.294) for Sindai. The QMM and EQMM models have low values of r and CE, high values of RMSE as compare to delta method. Taylor diagram between standard deviation, correlation coefficient and RMSE of delta method (DM), quantile mapping method (QMM) and empirical quantile mapping method (EQMM) which are presented in Fig. 1 to Fig. 3 for precipitation at Site_1, Site_2, Site_3, Site_4, Site_5, Site_6, Site_7, Site_8, Site_9, Site_10, Site_11, Site_12, Site_13, Site_14, Site_15, Amdi, Raipur and Singsai respectively.

It is observed from Taylor diagram of downscale methods that delta method indicates similar standard deviation to standard deviation of base precipitation, minimum RSME and maximum correlation coefficient. It is depicted from diagram that quantile mapping method (QMM) and empirical quantile mapping method (EQMM) indicates greater variation of standard deviation from standard deviation of observe runoff, greater RSME and less correlation coefficient as compare to delta method at Site_1, Site_2, Site_3, Site_4, Site_5, Site_6, Site_7, Site_8, Site_9, Site_10, Site_11, Site_12, Site_13, Site_14, Site_15, Amdi, Raipur and Singsai stations. Taylor diagram is a graphical comparison of different models with standard deviation, correlation coefficient and RMSE. It was exhibited from Taylor diagram that delta model has higher correlation, and lower standard deviation and RMSE values as compared to QMM and EQMM models in all stations. Therefore, delta method performed better than quantile mapping and empirical quantile mapping methods for downscaling of precipitation in all gauging stations. These results reveal that

there is an acceptable agreement between the station-observed precipitation data and downscale precipitation data.

The precipitation of the base period (1990-2013) and the future GCMs projections till the end of 2099 are presented in Fig. 4 to Fig. 6 for period of 1990-2013, 2020-2039, 2040-2059, 2060-2079 and 2080-2099 respectively. The projected distribution of these data series is presented on monthly basis. The base length of the ridges in Fig. 4 represents the precipitation distribution in each month and the height of these ridges stands for density of the data. The higher the height of a data point, the higher the value of density function. The distribution of the base period exhibits maximum precipitation during the month of July and August with a maximum precipitation of about 650 mm. In base period, January, February, March, April, May, November and December shows normal distributions whereas the precipitation data for all other months exhibits not a normal distribution. In Scenario (2020-2039), ridge lengths of July and August were about like base period while ridge length of September and June show small. In same way, ridge lengths of July and August were less than 600 mm whereas for base period more than 600 mm during July and August. The height of these ridges stands for density of the data. Higher the height of a data higher the value of density function.

In India, about 80% of annual precipitation is due to the southwestern monsoon between June and September. A small decreasing trend in the annual rainfall was observed across India, whereas a small increasing trend is observed in northwestern and peninsular India. In northeastern India, the highest rainfall-receiving region on the planet, no clear trend of rainfall for 1871–2008 was observed (Jain *et al.*, 2013). An increase in heavy rainfall events and decrease in low and

medium rainfall events were observed across India (Goswami *et al.*, 2006). In central India, a significant decreasing trend (10% significance level) of the mean of July and August rainfall was observed during 1951–2010 (Singh *et al.*, 2014). In several major river basins, the number of rainy days decreased while the number of intense events increased (Jain *et al.*, 2017). Average annual precipitation is expected to increase by 7–18.7% for various representative concentration pathways (RCPs) by 2099 compared with the 1961–1990 baseline using 18 Coupled Model Inter comparison Project Phase 5 (CMIP5) models across India (Chaturvedi *et al.*, 2012). In several river basins across India, precipitation is projected

to increase up to 30% in the mid-term (2040–2069) and 50% in the long term (2070–2099) from observed data for the period of 1971–2005 using five general circulation models (GCMs) of CMIP5 (Mishra and Lilhare 2016). It was recommended that delta method may be applied for downscale precipitation in future works. It may be applied in assessment of surface and ground water for planning and management, ground water recharge from canals and monsoon rainfall. For future research point of view, authors suggest that the accuracy and efficiency of downscaling of precipitation may be increased by applying soft computing method (Singh *et al.*, 2016a&b; 2017; 2018a&b, 2019).

Table.1 List of meteorological stations in upper Shivnath basin

S.No	Station Name	Source of data	Latitude (Degree)	Longitude (Degree)	Elevation
1	Amdi	CWC	21.068	81.567	268
2	Singdai	CWC	21.325	81.253	319
3	Raipur	IMD	21.237	81.709	287
4	Site_1	CFSR	20.763	80.938	359
5	Site_2	CFSR	20.763	81.250	314
6	Site_3	CFSR	20.763	81.563	308
7	Site_4	CFSR	21.075	80.938	297
8	Site_5	CFSR	21.075	81.250	278
9	Site_6	CFSR	21.075	81.563	279
10	Site_7	CFSR	21.388	80.938	321
11	Site_8	CFSR	21.388	81.250	280
12	Site_9	CFSR	21.388	81.563	278
13	Site_10	CFSR	21.700	80.938	451
14	Site_11	CFSR	21.700	81.250	304
15	Site_12	CFSR	20.763	80.625	346
16	Site_13	CFSR	21.075	80.625	358
17	Site_14	CFSR	20.451	81.250	405
18	Site_15	CFSR	21.388	81.875	290

Table.2 Comparison of various downscaling techniques for precipitation

Site	DM			QMM			EQMM		
	RMSE	CE	r	RMSE	CE	r	RMSE	CE	r
Site_1	10.056	0.350	0.647	10.547	0.211	0.587	11.550	0.041	0.502
Site_2	5.810	0.728	0.859	9.305	0.270	0.619	10.920	0.154	0.529
Site_3	7.590	0.513	0.725	10.075	0.076	0.479	9.157	0.050	0.503
Site_4	5.812	0.690	0.859	9.101	0.101	0.552	10.810	0.013	0.520
Site_5	5.819	0.735	0.863	10.487	0.220	0.576	10.589	0.050	0.525
Site_6	5.110	0.680	0.836	10.568	0.282	0.560	10.164	0.267	0.556
Site_7	7.930	0.595	0.779	10.789	0.076	0.500	10.870	0.175	0.528
Site_8	6.364	0.709	0.846	9.468	0.278	0.394	10.298	0.129	0.531
Site_9	6.933	0.409	0.736	10.248	0.139	0.513	10.533	0.132	0.509
Site_10	7.592	0.591	0.776	10.336	0.090	0.530	10.583	0.056	0.510
Site_11	7.411	0.606	0.787	8.686	0.281	0.546	9.157	0.101	0.503
Site_12	7.183	0.568	0.823	10.568	0.071	0.560	10.920	-0.037	0.542
Site_13	7.592	0.476	0.776	10.031	0.067	0.563	10.921	-0.069	0.529
Site_14	7.183	0.670	0.823	9.219	0.091	0.579	9.840	0.013	0.536
Site_15	7.411	0.390	0.787	8.375	0.325	0.734	9.811	0.310	0.656
Amdi	8.810	0.308	0.703	10.164	0.083	0.557	8.855	0.281	0.656
Raipur	9.352	0.351	0.537	9.824	0.187	0.610	11.554	0.041	0.502
Singdai	8.961	0.294	0.725	9.632	0.247	0.618	7.597	0.284	0.622

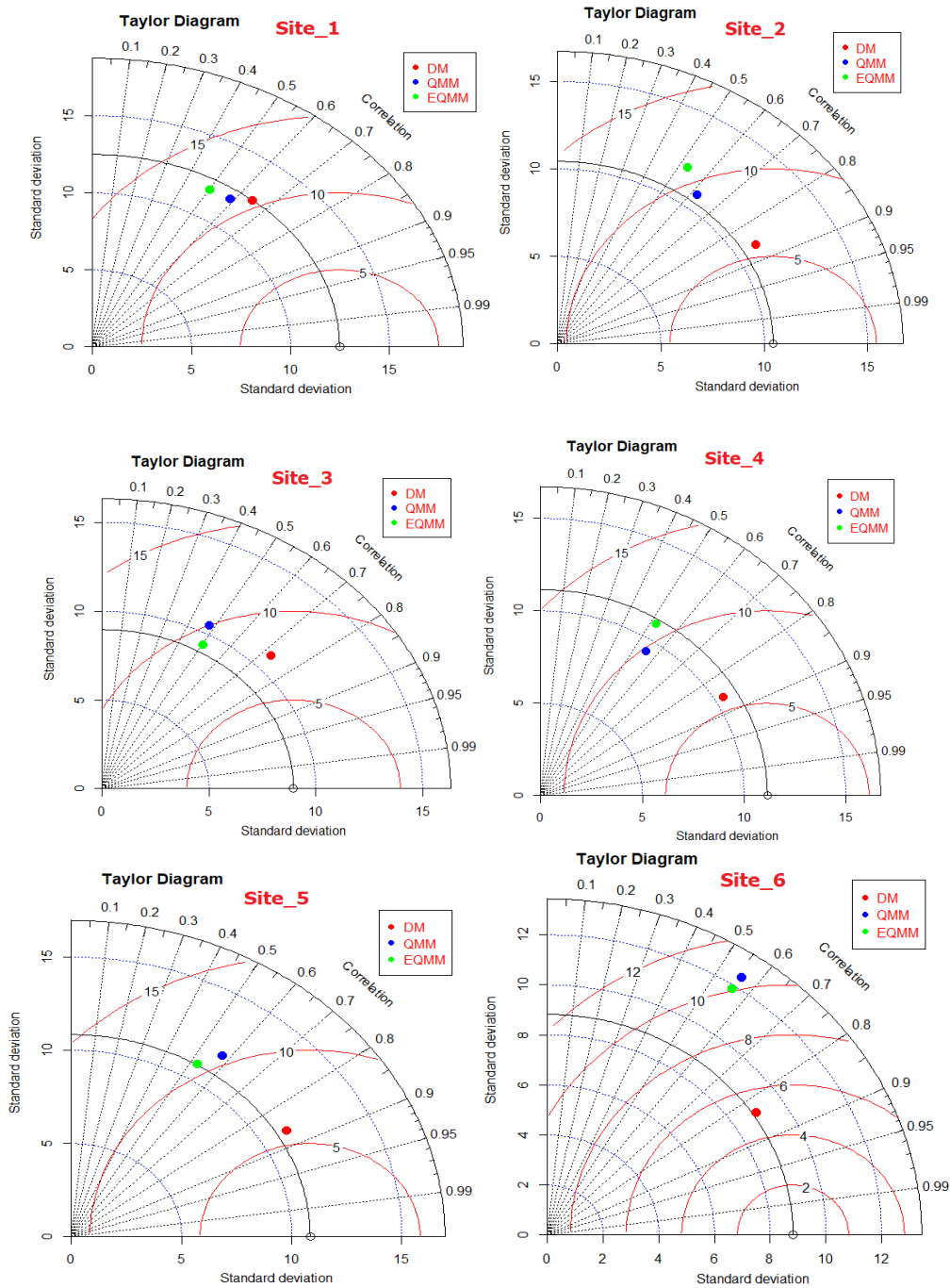


Fig.1 Taylor diagram of precipitation downscaling models for Site_1 to Site_6

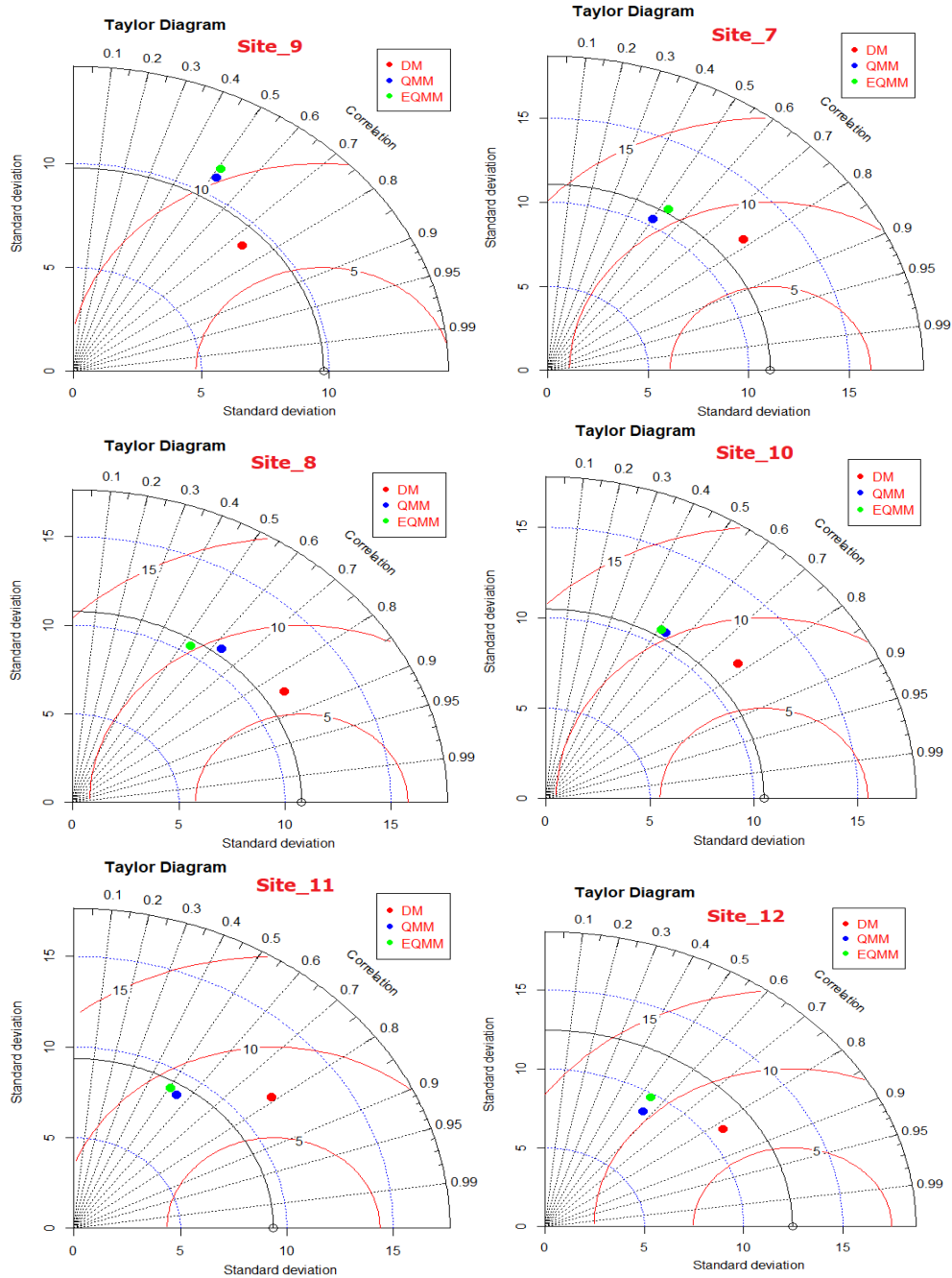


Fig.2 Taylor diagram of precipitation downscaling models for Site_7to Site_12

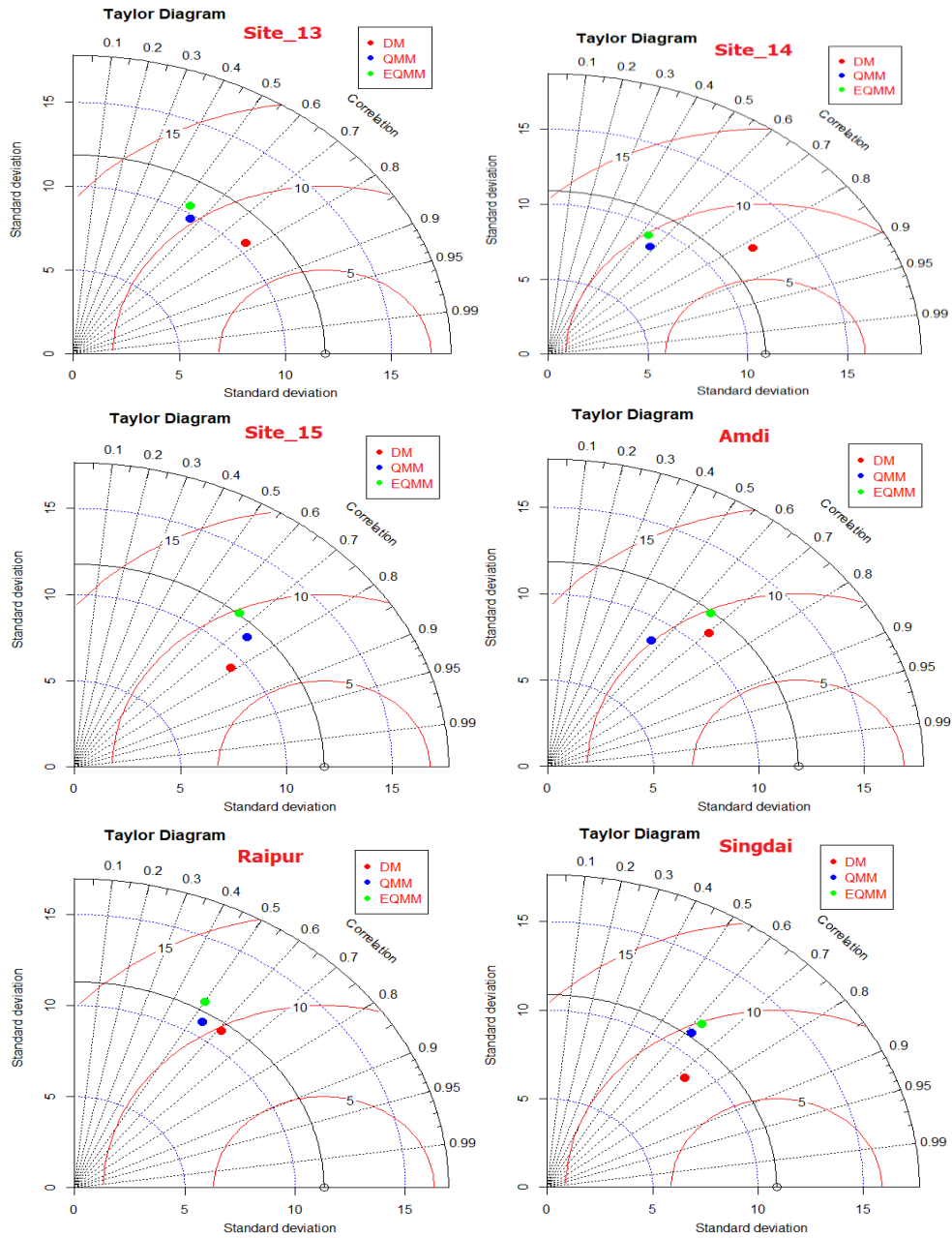


Fig.3 Taylor diagram of precipitation downscaling models for Site_13, Site_14, Site_15, Amdi, Raipur and Singdai

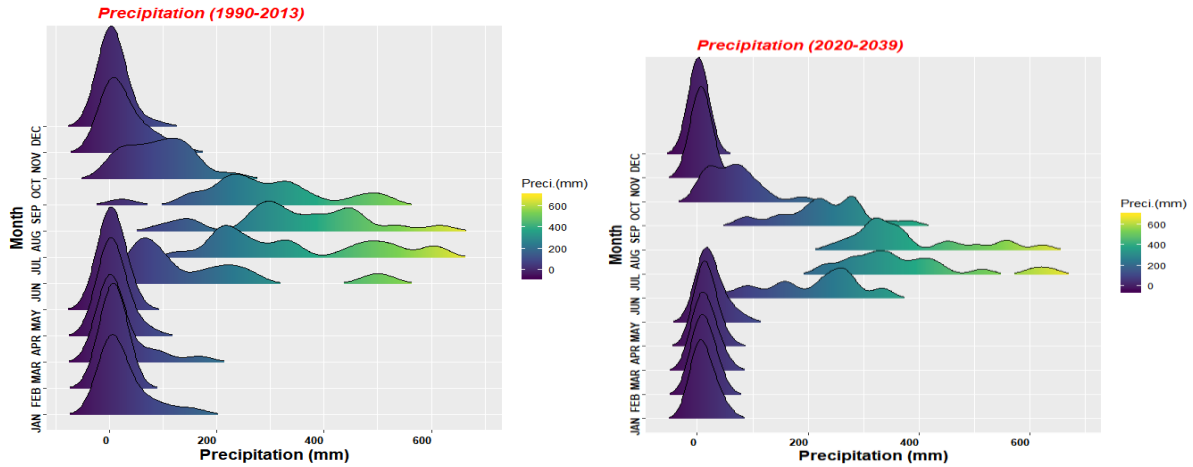


Fig.4 Precipitation distribution of base (1990-2013) and future (2020-2039) periods

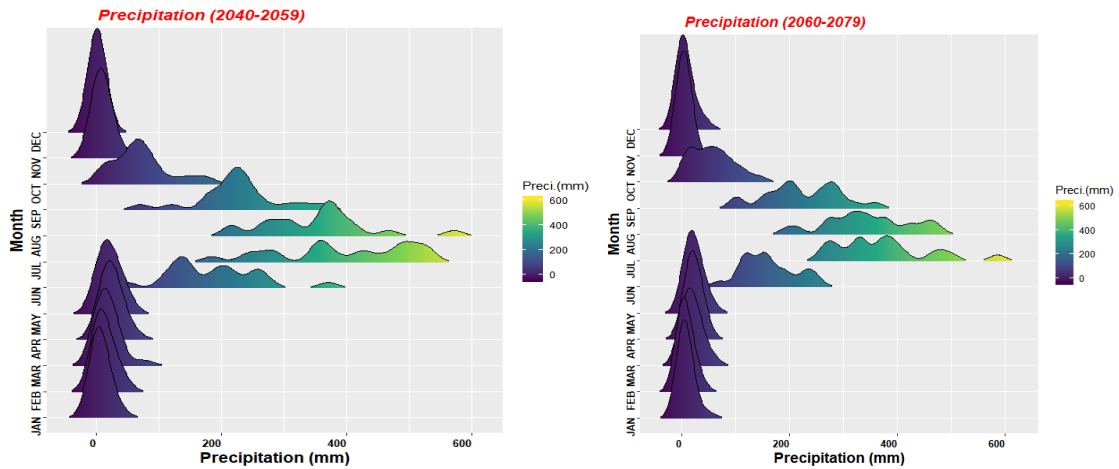


Fig.5 Precipitation distribution of future a (2040-2059) and (2060-2079) periods

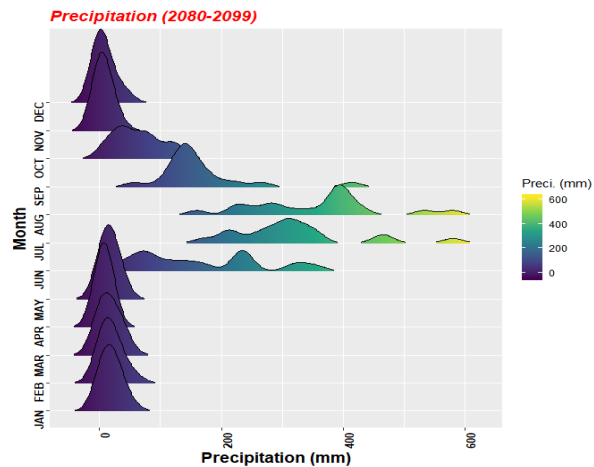


Fig.6 Precipitation distribution for future (2060-2079) periods

Summary and conclusions

The observed dataset for baseline period (1990-2013) was collected from department of agrometeorology, Indra Gandhi Krishi Vishwavidyalaya, Raipur, Chhatisgarh, India, regional office of IMD and CWC, Raipur, Chhatisgarh, India. Model for Interdisciplinary Research on Climate 5 (MIRCO5) simulation model was used for future Representative Concentration Pathways (RCP) scenarios (RCP4.5) to project decadal changes in across eighteen selected stations of Upper Shivnath basin. Three decades were selected for future prediction viz. 2020–2039, 2040–2059, 2060–2079 and 2080-2099 and were compared decadal variabilities with period 1990–2013. Delta method is accurately downscale precipitation from Model for Interdisciplinary Research on Climate (MIRCO5) model for future Representative Concentration Pathways (RCP) scenarios (RCP4.5) to project decadal changes in precipitation across eighteen selected stations of Upper Shivnath basin as compare to quantile mapping and empirical quantile mapping methods. The downscale precipitation across eighteen selected stations of Upper Shivnath basin from Model for Interdisciplinary Research on Climate (MIRCO5) model for 2020-2039, 2040-2059, 2060-2079 and 2080-2099 scenarios are observed decrease trend in future. The rainfall pattern of Upper Shivnath basin is showing a decreasing trend with time. While, industrialization and population growth in the basin, especially in Raipur, Bilai and Rajnandgav region is dramatically increasing, ground water recharge is decreasing on account of decrease in rainfall on the one hand and excessive demand of water on the other hand. This would create severe water crisis in future. To arrest this situation rainwater harvesting is a viable solution.

Acknowledgement

Author give special thanks to TEQIP-III for financial support.

References

- Bettolli, M. L., & Penalba, O. C. 2014. Synoptic sea level pressure patterns-daily rainfall relationship over the Argentine Pampas in a multi-model simulation. *Meteorological Applications*, 21, 376–383.
- Chaturvedi, R. K., Joshi, J., Jayaraman, M., Bala, G. and Ravindranath, N. H. 2012. Multi-model climate change projections for India under representative concentration pathways, *Curr. Sci.* 103 (7): 791–802.
- Giorgi, F., & Mearns, L. O. 1991. Approaches to the simulation of regional climate change: A review. *Reviews of Geophysics*, 29, 191–216.
- Goswami, B. N., Venugopal, V. Sengupta, D. Madhusoodanan, M. S. and Xavier, P. K. 2006 Increasing trend of extreme rain events over India in a warming environment, *Science* 314 (5804): 1442–1445.
<https://doi.org/10.1126/science.1132027>
- Huth, R., Miksovsky, J., Stepanek, P., Belda, M., Farda, A., Chladova, Z., & Pišoft, P. 2015. Comparative validation of statistical and dynamical downscaling models on a dense grid in central Europe: Temperature. *Theoretical and Applied Climatology*, 120, 533–553. <https://doi.org/10.1007/s00704-014-1190-3>
- Jain, S. K., Kumar, V. and Saharia. M. 2013. Analysis of rainfall and temperature trends in northeast India, *Int. J. Climatol.* 33 (4): 968–978. <https://doi.org/10.1002/joc.3483>.
- Jain, S. K., Nayak, P. C. Singh, Y. and Chandniha, S. K., (2017) Trends in rainfall and peak flows for some river basins in India, *Curr. Sci.* 112 (8): 1712. <https://doi.org/10.18520/cs/v112/i08/1712-1726>.
- Maenza, R., AgostaScarel, E. A., & Bettolli, M. L. 2017. Climate change and precipitation

- variability over the western “Pampas” in Argentina. *International Journal of Climatology*, 37, 445–463. <https://doi.org/10.1002/joc.5014>
- Meehl, G. A., Covey, C., Delworth, T. L., Latif, M., McAveney, B., Mitchell, J. F. B., Taylor, K. E. 2007. The WCRP CMIP3 multimodel dataset: A new era in climate change research. *Bulletin of the American Meteorological Society*, 88, 1383–1394. <https://doi.org/10.1175/BAMS-88-9-1383>
- Mishra, V., and Lihare. R. 2016. Hydrologic sensitivity of Indian subcontinental river basins to climate change, *Global Planet. Change* 139:78–96. <https://doi.org/10.1016/j.gloplacha.2016.01.003>.
- Rummukainen, M. 2010. State-of-the-art with regional climate models. *WIREs Climate Change*, 1, 82–96. <https://doi.org/10.1002/wcc.8>
- Silvestri, G., & Vera, C. 2008. Evaluation of the WCRP-CMIP3 model simulations in the La Plata Basin. *Meteorological Applications*, 15, 497–502. <https://doi.org/10.1002/met.98>
- Singh VK, Kumar D, Kashyap PK, Kisi, O. 2018b. Simulation of suspended sediment based on gamma test, heuristic, and regression-based techniques. *Environ Earth Sci.* <https://doi.org/10.1007/s12665-018-7892-6>
- Singh VK, Kumar P, Singh BP. 2016b. Rainfall-runoff Modeling using Artificial Neural Networks (ANNs) and Multiple Linear Regression (MLR) Techniques *Ind J Eco* 43 (2): 436-442
- Singh VK, Singh BP, Kisi O, Kushwaha, DP, 2018a. Spatial and multi-depth temporal soil temperature assessment by assimilating satellite imagery, artificial intelligence and regression-based models in arid area. *Comput Electron Agric.* <https://doi.org/10.1016/j.compag.2018.04.019>
- Singh, D., Gupta, R. D. and Jain. S. K. 2014. Study of long-term trend in river discharge of Sutlej River (NW Himalayan region). *Geogr. Environ. Sustainability* 7 (3): 87–96. <https://doi.org/10.24057/2071-9388-2014-7-3-87-96>.
- Singh, V.K., Kumar, D., Kashyap, P.S., Singh, P.K., Kumar, A., Singh, S.K. 2019. Modelling of soil permeability using different data driven algorithms based on physical properties of soil, *Journal of Hydrology* <https://doi.org/10.1016/j.jhydrol.2019.124223>
- Singh, V.K., Singh, B.P., Kumar, A., Vivekanand, 2017. A comparative study of artificial intelligence and conventional techniques for rainfall-runoff modeling *Int. J. Agril. Eng.* 10 (2), 1–9. <http://dx.doi.org/10.15740/HAS/IJAE/10.2/441-449>
- Singh, V.K., Singh, B.P., Vivekanand, 2016a. Basin suspended sediment prediction using soft computing and conventional approaches in India. *Int J Sci Natur* 7 (2), 459–468.
- Wilby, R. L., Charles, S. P., Zorita, E., Timbal, B., Whetton, P., & Menéndez, C. G., de Castro, M., Boulanger, J.-P., D’Onofrio, A., Sanchez, E., Sörensson, A. A., ... Teichmann, C. 2009. Downscaling extreme month-long anomalies in southern South America. *Climatic Change*, 98, 379–403. <https://doi.org/10.1007/s10584-009-9739-3>

How to cite this article:

Vijay Kumar Singh and Devendra Kumar. 2020. Downscaling daily precipitation over the Upper Shivnath basin: A comparison of three statistical downscaling techniques. *Int.J.Curr.Microbiol.App.Sci.* 9(01): 1676-1688. doi: <https://doi.org/10.20546/ijcmas.2020.901.185>